Check for
updates

Identifying and contrasting the sources of the water vapor reaching the subregions of the Tibetan Plateau during the wet season

Bin Chen[1] · Wei Zhang[2] · Shuai Yang[3] · XiangDe Xu[1]

Abstract

A Lagrangian approach is utilized to identify and compare the sources of water vapor transported to the four subregions of Tibetan Plateau (TP) during the wet season (May–August) of 1980–2016. We focus on the time scale and subseasonal variability of water vapor transport and the relationship between moisture supply and precipitation at the interannual scale. This study finds that: (1) The moisture sources for the four subregions differ significantly in both spatial pattern and magnitude and depend heavily on the combined effects of the summer monsoons, local recycling and the westerlies. (2) The spatial evolution of the moisture sources based on the backward trajectory analysis reveals that, although approximately 80% of the moisture is delivered to the target regions within 1–4 days, the individual subregions feature different transport pathways and associated time scales. (3) The subseasonal migration of the Indian summer monsoon regulates the importance of different moisture sources for the southern TP but not for the northern TP. Additionally, the subseasonal moisture source evolution differs greatly between the southeastern TP and the southwestern TP. (4) The interannual variability of precipitation over the whole TP during summer is negatively correlated with the variation in the moisture transported by the westerlies and is positively related to the moisture conveyed by the Indian summer monsoon for the northern TP and by adjacent moisture transport for the southern TP.

1 Introduction

The Tibetan Plateau (TP) also known as 'the global water tower' or 'the third pole' is the highest plateau in the world and exerts profound effects on regional and global weather and climate systems (Wu et al. 2007; Xu et al. 2008; Yao et al. 2013). The changing climate system can also impact the TP's regional climate, especially precipitation variability, threatening the hydrological cycle over many regions, potentially impacting the fresh water availability of more

✉ Wei Zhang
  wei-zhang-3@uiowa.edu

1 State Key Laboratory of Severe Weather, Chinese Academy of Meteorological Sciences, Beijing 100081, China

2 IIHR-Hydroscience and Engineering, The University of Iowa, Iowa City, IA, USA

3 Laboratory of Cloud-Precipitation Physics and Severe Storms (LACS), Institute of Atmospheric Physics, Chinese Academy of Sciences, Beijing 100029, China

than 1.4 billion people downstream (Immerzeel et al. 2010; Yang et al. 2014; Wang et al. 2018). Therefore, research on the hydrological cycle over the TP has aroused interest worldwide because of considerable societal ramifications (Bolch et al. 2012; Yao et al. 2013; Yang et al. 2014; Bibi et al. 2018; Bookhagen and Burbank 2010; Ma et al. 2018).

As one of the most active components of the hydrological cycle, the supply of atmospheric moisture has been regarded as a bridge between the influencing factors and the resultant regional climate change (Gimeno et al. 2010a). It has been well established that the Indian/Eastern Asian summer monsoon delivers abundant moisture from the remote tropical oceans to the TP during the boreal summer (Xu et al. 2014; Dong et al. 2016), while the mid-latitude westerlies also deliver a fraction of the moisture to the northern TP (Bothe et al. 2012; Yao et al. 2013; Zhang et al. 2017). These large-scale atmospheric circulation patterns and associated water vapor transport significantly affect summer precipitation over the TP (Bothe et al. 2012; Chen et al. 2012; Curio et al. 2015; Maussion et al. 2014). Hence, the quantitative identification of the sources of water vapor over the TP can lead to a better understanding of the precipitation variability

over the TP and facilitate the management of risks and water supplies under a changing climate (Yang et al. 2014).

In fact, a number of studies have been conducted to identify and quantify the sources of moisture over the different parts of the TP with a wide range of methods. For instance, based on the analysis of the water vapor flux, Feng and Zhou (2012) showed that the moisture originating from the Indian Ocean and the Bay of Bengal dominated the summer moisture in the southeastern TP during 1979–2002. Using the Lagrangian tracking approach, Chen et al. (2012) examined the primary source of water vapor over the main body of the TP for the boreal summers of 2005–2009 and identified a relatively narrow belt, ranging from the northwestern TP to the Indian subcontinent to the Southern Hemisphere. Using a similar method, Sun and Wang (2014) identified the Eurasian continent as the predominant contributor to the eastern TP during the summers of 2000–2009. More recently, Dong et al. (2016) documented moisture transport from central-eastern India to the southwestern TP conveyed by deep convection and mid-tropospheric circulation during the summer. Zhang et al. (2017) and Pan et al. (2018) recently explored the moisture sources for the central-western TP and the southern TP, and they highlighted the roles of the Eurasian continent and the tropical Indian Ocean in supply moisture to these two regions, respectively. In addition to studies on exact moisture source identification, the relative contributions of remote moisture sources versus local recycling have also been explored. For instance, Curio et al. (2015) suggested that less than 40% of the precipitation over the TP originates from external moisture sources, while the remaining percentage ($>60\%$) originates from local moisture recycling. Yang et al. (2014) suggested that continental recycling is an important moisture source over the central and northern TP, while the Indian Ocean is the prevailing moisture source for the southern TP by analyzing isotopic data.

Most of the aforementioned studies provide valuable insights into understanding the atmospheric hydrological cycle over the TP; however, the exploration of the determination of the moisture sources to the TP is still in its early stages, and there is no consensus on the quantification of the contributions of different moisture sources to the water vapor over the TP. More importantly, four primary climate processes are commonly acknowledged to regulate moisture transport to the TP: the Indian monsoon system, the mid-latitude westerlies, the East Asian monsoon system and local moisture recycling (Xu et al. 2008; Yao et al. 2013). Because of the complexity in the climate system and the large spatial extent of high-elevation terrain (covering approximately 2.5×10^6 km^2), precipitation dramatically decreases from the southeastern TP to the northwestern TP, generating significant spatial heterogeneity. Yao et al. (2013) highlighted that the northern TP is mainly influenced by the westerlies,

while the southern TP is controlled by the Asian summer monsoons. Even along the same latitudinal belt, the atmospheric circulation patterns (Dong et al. 2016) and the surface heat fluxes (Ma et al. 2006; Li et al. 2013; Zhong et al. 2019) regulating the moisture transport to the western TP are different from those for the eastern TP. All these factors hamper a general conclusion regarding the identification of the moisture source. This is particularly true for the studies that only focused on a single predefined subregion of the TP or examined relatively short periods (Chen et al. 2012; Sun and Wang 2014).

Although major progress has been made, the moisture sources and their quantitative contributions to the water vapor remain unclear for the TP and its subregions: northwestern TP (NWTP), northeastern TP (NETP), southeastern TP (SETP), and southwestern TP (SETP). Furthermore, the differences in the relationship between moisture and precipitation over the subregions of the TP might provide physical mechanisms responded for precipitation variability, which has not been systematically explored yet. Therefore, this study aims to quantify the climatological sources of the water vapor reaching the TP during the summer season (May–August), to compare the moisture sources for different subregions over the TP, and to explore the differences in interannual changes in precipitation and the underlying physical mechanisms.

The remainder of this paper is organized as follows. The model, data, and methods are provided in Sect. 2. The principal results, including the climatology of moisture sources for different subregions, their evolution based on backward trajectories, and the subseasonal variation, together with their relevance to the interannual variability over the TP, are presented in Sects. 3.1–3.4, respectively. Section 4 presents the discussion. Finally, conclusions are provided in Sect. 5.

2 Data, model, and methods

2.1 Data

The boundary forcing of the Lagrangian model is obtained from the European Centre for Medium-Range Weather Forecasts reanalysis (ERA)-Interim data (Dee et al. 2011), which performs better than other reanalysis data sets in modeling the atmospheric water cycle over the TP (Gao et al. 2014). The meteorological fields contained in the ERA-Interim data are in 60 hybrid model levels from the ground to 0.1 hPa with a longitude/latitude grid resolution of $0.75° \times 0.75°$ at the 6-hour time step. The study period covers May to August of 1980–2016.

We use monthly $0.25° \times 0.25°$ gauge-based rainfall data, which are derived from more than 2400 gauge stations across mainland China and obtained from the National

Meteorological Information Center of the China Meteorological Administration (NMIC/CMA) for the period of 1980–2014. This data set has been extensively used to investigate East Asian monsoon precipitation.

2.2 Lagrangian model and running setup

A relatively sophisticated diagnostic Lagrangian scheme developed by Stohl and James (2004, 2005) was used to quantify the source of the water vapor reaching the TP. The Lagrangian approach provides more realistic traces of air parcels, for following trajectories and establishing source–sink relationships. The Lagrangian transport and dispersion model (FLEXPART, V9.02) was used to perform the multiyear modeling to generate the simulation data set for further use in moisture source identification. This model has been widely used to study the atmospheric water vapor transport, particularly for the identification of moisture sources/sinks (Drumond et al. 2008; Gimeno et al. 2010b; Nieto et al. 2010; Sodemann et al. 2008; Sun and Wang 2014; Chen et al. 2012, 2018).

Because the annual total precipitation over the TP is dominated by that during the summer season, we focus on the period from May to August (MJJA). The regional volume of atmospheric air mass (15°S–60°N and 0–160°E) was homogeneously separated into ~ 1.4 million air parcels. The modeling period is set from 15 April to 15 September for each summer season. Information on the specific humidity, three-dimensional positions (longitude, latitude, and height), temperature, etc. were recorded at 6-hour intervals for each air parcel. Eventually, a 6-hourly Lagrangian modeling output data set from 1980 to 2016 (37 years) was constructed. This relatively long data set allows for a robust diagnosis of the climatological characteristics of the sources of the water vapor reaching the TP and the relationship between moisture supply and precipitation upon multiple temporal scales.

2.3 Methodology to determine the moisture sources

Based on the multiyear output of the Lagrangian modeling, the backward tracking approach is used to quantify the sources of the water vapor that reached individual subregions of the TP. Different from previous studies, our main aim of this study is to determine and characterize the external moisture sources that affect the four predefined subregions (the NWTP, NETP, SWTP, and SETP). Thus, only those ensemble external trajectories are selected for further backward tracking analysis. The external trajectories are defined as the air parcels that entered each of the four predefined subregions at each 6-hour time step from regions outside of the TP domain (the regions with the elevation higher more than 2500 m). Since only the external air parcels are considered, the contribution to the moisture by the processes of local recycling over the TP are, to some extent, excluded in this study. This selection criterion can exclude air parcels within the TP region itself but does not consider whether the air parcels produce precipitation after entering the TP. The external trajectories are selected every 6 h from 1 May to 31 August during 1980–2016. All trajectories are tracked backward for 10 days, which is equal to the average residence time of water vapor in the atmosphere (Numaguti, 1999; Gimeno 2012).

For the single selected trajectory, the method calculates increases (e) and decreases (p) in moisture along each trajectory via changes in (q) at each time step, i.e. $(e–p) = m \cdot dq/dt$. By counting the number of trajectories and summing (e–p) for all particles existing in the atmosphere, we obtain (E–P) fields, where E and P are the rates of evaporation and precipitation, respectively. In the two-dimensional (E–P) fields, the sources are identified as those regions with positive (E–P) values. Finally, the (E–P) > 0 fields from all tracks are aggregated to a regular $1.0° \times 1.0°$ grid and aggregated separately to daily, monthly, and seasonal (May–June to July–August) intervals, which allows to explore the spatial and temporal variability and the association with summer rainfall. More details on the moisture source diagnosis are described in Stohl and James (2005) and Gimeno (2012).

Once the air parcels gain moisture in a particular region, they lose some or all of the moisture along their trajectories before they reach the target regions due to the processes of precipitation. Thus, the previous contributions by the moisture sources needed to be rescaled for each particle. To quantify the influence of these physical processes on the source regions, we reestimate the fractional contribution of each source. Along the individual journey of the backward tracking, the moisture increases at the n-th uptake locations with their unweighted contribution $\Delta q_n = q_{n+1} - q_n$ was initialized firstly, where q_{n+1} and q_n are the specific humidity of the air parcel at uptake location before and after the 6-hour interval, respectively. Under the simplifying assumptions that (1) in case of $\Delta q < 0$ all moisture decrease is due to precipitation and (2) there are *m* precipitation events in total at the nth uptake locations along the backward tracking before they reach the subregions of the TP. Considering the precipitation events would reduce the importance of previous uptakes, the contribution of moisture uptakes at n-th uptake location with respect to the specific humidity are recalculated by

$$\Delta q'_n = \Delta q_n \times \sum_{i=1}^{m} \left(\frac{q_{i+1}}{q_i} \times 100\% \right)$$

This recalculation took the possibility of multiple precipitating events along the individual trajectories into account, which similar to the the method of Sodemann et al. (2008)

and Chen and Xu (2016) by considering the possibility of multiple rounds of recycling.

3 Results

3.1 Summer mean moisture sources

Figure 2 exhibits the climatological (37 years) seasonal mean of the integrated moisture sources, i.e. (E–P) > 0 of days 1–10 for individual subregions. This figure illustrates the average of all gains of moisture over the previous 10 days. It is not surprising that most water in the TP is supplied from upwind evaporation source areas, but the trajectories become more dispersed in areas farther upstream. Overall, the aggregated perspective for all subregions suggests that the predominant moisture sources are located in neighboring continental areas that are not far from each target region. In this sense, the surrounding terrestrial regions, including part of the target region itself, tend to be the primary regions that contribute the most moisture. The dominant role of terrestrial moisture in the water supply of the TP has been documented in previous studies (e.g., Feng and Zhou 2012; Yao et al. 2013; Curio et al. 2015).

Furthermore, it is obvious that the spatial patterns of moisture contribution for four subregions exhibit large differences between the northern TP (the NWTP and NETP) and the southern TP (the SWTP and SETP). In particular, the moisture in the northern TP from more remote sources is mainly supplied from the Eurasian continent (Fig. 2a, c), while the moisture in the southern TP is largely supplied from subtropical and tropical regions (Fig. 2b, d). Considering the dominant atmospheric circulation systems regulating the moisture transport to the TP, we can deduce that

the remote water supply for the northern TP is more likely influenced by land-surface evaporation and the mid-latitude westerlies, as the mean moisture distribution extends latitudinally. However, the remote moisture sources for the southern TP tend to be mainly influenced by the Indian summer monsoon because their distribution pattern is consistent with this atmospheric circulation pattern (Fig. 1, vector). The remote moisture sources for the southern TP are characterized by a narrow band in the tropical–subtropical Arab Sea corridor, stretching southward from the Indian subcontinent to the Southern Hemisphere, which is consistent with the findings of previous studies (e.g., Chen et al. 2012; Zhang et al. 2017). Additionally, due to the inherent nature of the topography and dominant atmospheric circulation patterns, the moisture source distributions in the western and eastern parts of the TP are also dramatically different.

For a better comparison of moisture sources among the four subregions, we further take an integrated perspective by adding all values of the moisture sources in each grid in the longitude and latitude directions (Fig. 3a, b). The magnitude of values in Fig. 3 indicates the relative importance of the moisture sources, and a relatively wider band of peak values indicates a larger region of moisture sources covered and the opposite is true. Comparatively, the SETP receives the largest amount of moisture from a larger area, followed by the SWTP and NWTP, with the NETP receiving the least moisture. Although some differences exist in the magnitude of moisture sources for the SWTP and NWTP region, the spatial patterns of source areas are generally similar in space. The weak and narrow bands of peak values for the NETP again indicate the dominant role of neighboring areas in the water supply of this region. The double-peak structure, especially for the NWTP, suggests that this region features the combined influenced of multiple circulations regimes. The

Fig. 1 The topographical distribution (color shaded) with domains and abbreviations of the four subregions of interest. Here, the elevations greater than 2500 m are divided into four climate zones by the point (90°E, 33°N), i.e., the northwestern TP (NWTP), the northeastern TP (NETP), the southeastern TP (SETP), and the southwestern TP (SWTP). The arrow vectors indicate the vertically integrated water vapor flux derived from ERA-Interim (MJJA, 1980–2016, vector, in kg·m^{-1}·s^{-1}). The black thick contour indicates the elevation of 2500 m

Integrated (E-P)>0 of day 1-10
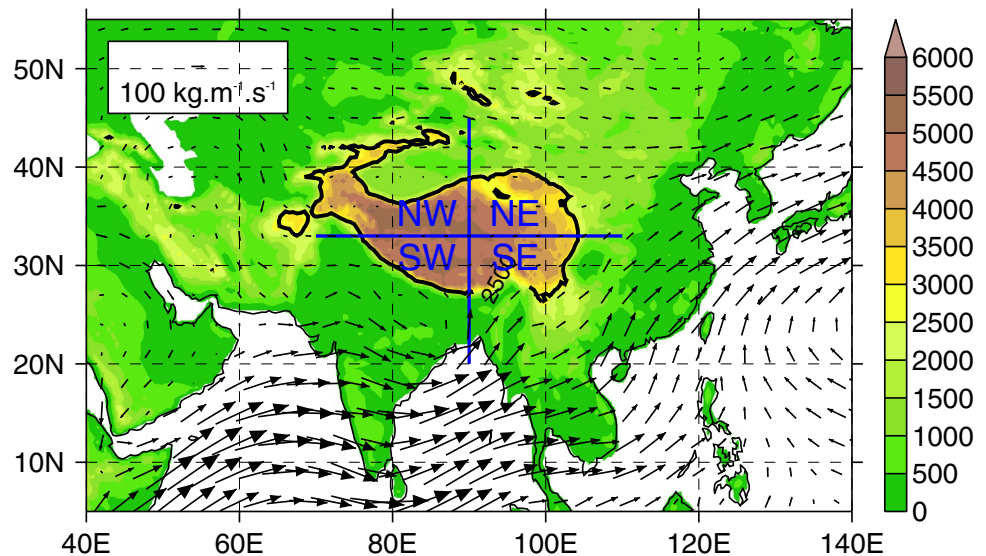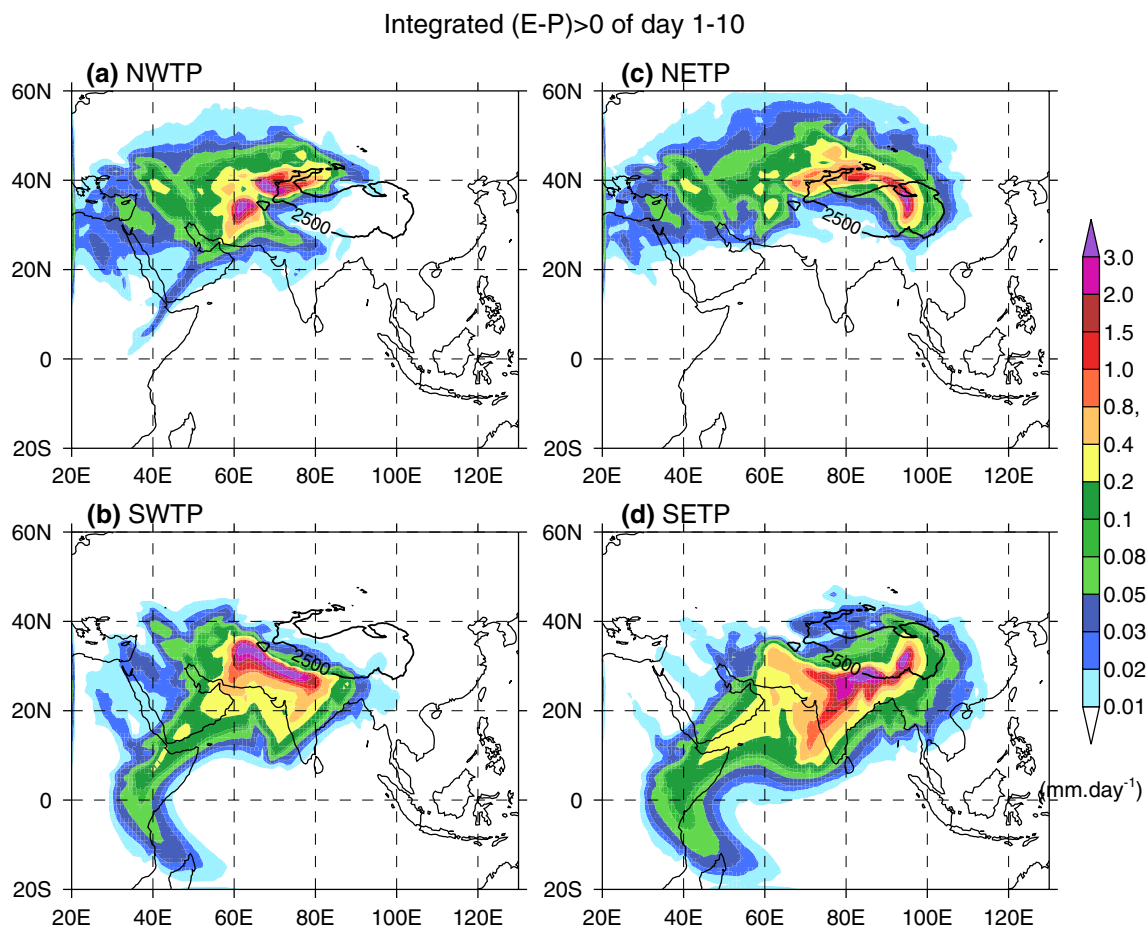
Fig. 2 The climatological seasonal evaporative moisture sources, i.e., the 10-day integrated (E–P) > 0, during the boreal summer of 1980–2016 (in mm day^{-1}) obtained via backward tracking of all the particles reaching the four subregions of **a** the NWTP, **b** NETP, **c** SWTP, and **d** SETP, respectively. The black thick contour indicates the 2500 m elevation

remarkable differences in magnitude and spatial distribution among the four subregions show that different climatic systems play different roles in determining the moisture sources for the four subregions of the TP.

For a more quantitative analysis on the dependency of moisture sources on the transport distance, we categorized the moisture sources into nine categories according to the distance between the moisture sources and their target region. The relative contribution of each category as a function of distance to their target region is illustrated in Fig. 3c. For the NETP, moisture sources with transport distances of no more than 200 km contributed approximately 25% of the water vapor, which again emphasize the roles of nearby vapor uptake or neighborhood recycling in the water supply. For the NWTP and SWTP, moisture sources at distances of 500–1500 km make the largest contribution, accounting for more than 50% while the contributions from other categories is small. Therefore, the moisture sources for the two regions are more concentrated (Fig. 2). Note that moisture sources with transport distances of less than 200 km are much less

important in the SWTP than in other subregions, probably arising from the unique water transport over this subregion. We will further discuss the mechanisms underpinning the water transport over this subregion in Sect. 3.2. The analysis of the SETP suggests that the relative contributions of different categories have similar magnitudes, suggesting that the moisture sources are widely dispersed (Fig. 2).

## 3.2 Moisture transport pathways and associated time scales

The Lagrangian diagnostic not only quantifies the spatial structure of the moisture source regions, it can also determine the exact time when the moisture uptake occurred along the journey of each air parcel to the target region. In this section, the temporal evolution of the moisture source with the backward tracking day is discussed. Figure 4 shows the distribution of the summer mean moisture sources for the SETP region for 1–9 days. Note that, for the backward tracking, here the day 1 represent the

Fig. 3 The **a** latitudinal and **b** longitudinal accumulated grid values of 10-day integrated (E–P) > 0, derived from the climatological seasonal average of boreal summer 1980–2016 (shown in Fig. 2), together with **c** the relative contribution of each moisture source category as a function of distance from the four target regions. The moisture sources are divided into nine categories according to the distance between the location of the moisture source and the target regions. The orange, blue, green and red lines in **a** and **b** represent the SETP, SWTP, NETP and NWTP regions, respectively
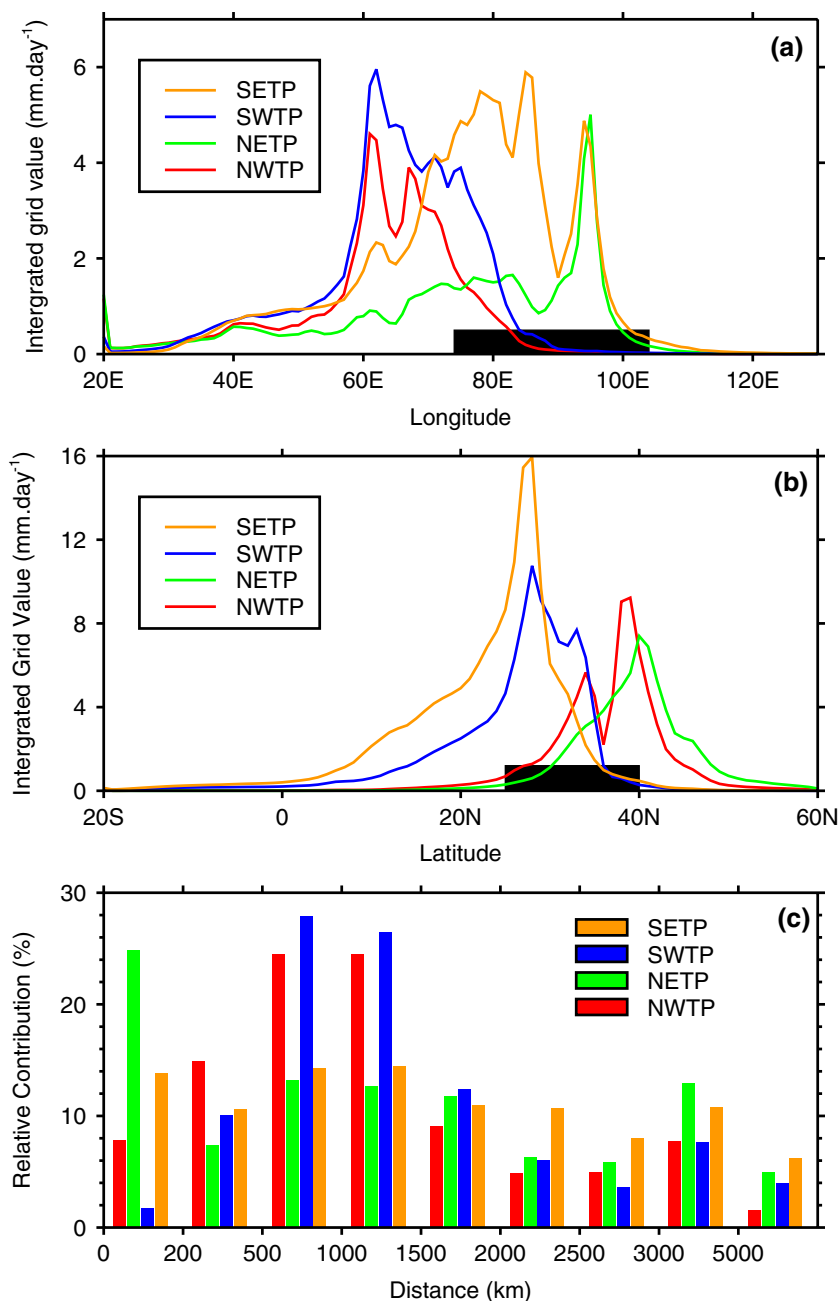
particles 1 day before the particles reach the TP (starting from closer areas) Despite the fact that the spatial evolution of the climatological summer mean moisture source with the backward tracking time does not represent the real moisture transport trajectories, they roughly reflect the pathways of water vapor transport to the sink regions. On the first day, the SETP and its neighboring regions within a relatively short distance to the target region were the major moisture sources. Because only the external trajectories reaching the target regions are selected here, the obvious water supply derived from the local region indicates that a number of air parcels might

have departed the target region first and then returned, creating local recycling in the moisture supply. For days 2–4 (Fig. 4b–d), the dominant moisture sources gradually extend to the entire Indian subcontinent. A similar distribution pattern can be observed on days 5–7 when there is a noteworthy southward expansion from the northern Indian subcontinent to the Arabian Sea and a decrease in the northeastern TP (Fig. 4e–g). On days 8–9 (Fig. 4h–i), the large moisture contributions from the Arabian Sea and the northwestern part of the Indian subcontinent remain steady, but a southward shift and a cross-equator moisture supply are also observed, confirming that the water vapor
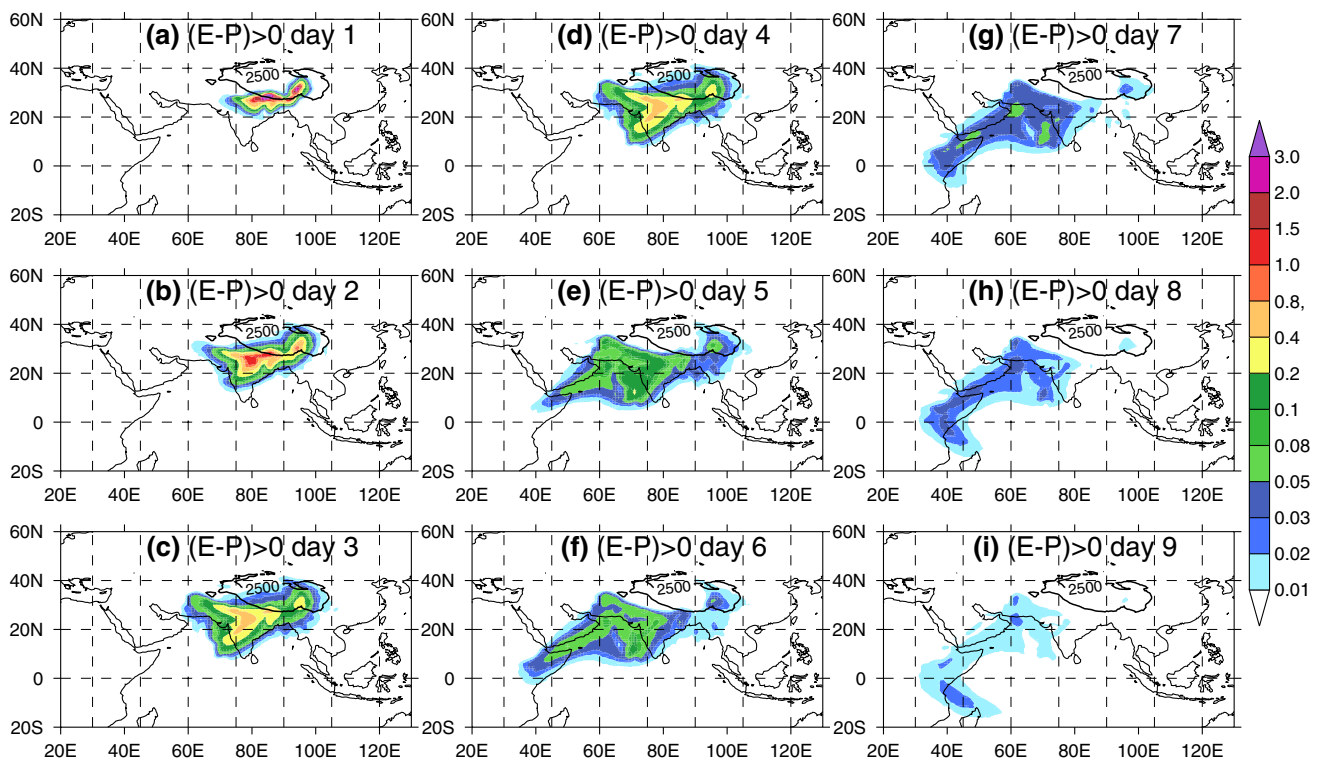
Fig. 4 Same as Fig. 2d, but for the climatology of the summer (MJJA) seasonal evaporative moisture sources of SETP region for separated backward tracking days 1–9, respectively. *SETP* southeastern Tibetan Plateau. The black thick contour indicates the 2500 m elevation

and precipitation over the SETP are partly influenced by cross-equator water transport (e.g. Xu et al. 2008; Chen et al. 2012; Zhang et al. 2017).

For the SWTP region, the evolution of summer mean moisture sources with backward tracking time (Fig. 5) is similar to that of the SETP (Fig. 4), particularly for the moisture supply with a relatively long transport timescale of 7–9 days. However, a closer look also reveals notable differences. First, the moisture source regions for the SWTP are distinctly separated spatially from the SWTP region itself. This gap means that, in contrast to the SETP, most air parcels leaving the SETP are less likely to return to this region during their subsequent journeys. Additionally, compared to the SETP, the moisture sources of the SWTP during 1–6 days in the backward tracking are more concentrated over the northern Indian subcontinent, with less contribution from the Arabian Sea. Considering the obstruction generated by the high topography of the Himalayas, there is no doubt that this characteristic is closely related to the special water vapor transport mechanisms over the SETP. Recently, Dong et al. (2016) reported that the SWTP tends to be influenced by water vapor transported from the northern Indian subcontinent through an "up-and-over" moisture transport system dominated by deep convection and mid-tropospheric circulation during the summer. The mechanisms proposed in Dong et al. (2016) are consistent with the findings of this study.

In contrast to the southern TP, the corresponding evolution of moisture sources with backward tracking time for the NWTP (Fig. 6) spanned a relatively small spatial extent and did not expand significantly with backward tracking time. The moisture sources cover the largest region on the fourth day beyond which the moisture sources shrink remarkably in space and weaken in magnitude, suggesting that the remote sources make only a minor contribution. The weak but substantially steady existence of a localized moisture source on days 7–9 also confirms that the water supply from neighboring regions is persistent and contributes considerable water vapor to this region. The evolution for the NETP (Fig. S1 in the supporting information) shows the same overall characteristics as for the NWTP but with a more significant contribution from the neighboring region (Fig. 3c).

To gain further insights into the characteristics of the moisture source with respect to transport time, we examine the temporal variation in the accumulative (E–P) > 0 for each backward tracking day by added the values on each grid and corresponding relative contributions to the four subregions (Fig. 7). The amount of moisture transported to the southern TP (the SETP and SWTP) is much larger than what transported to the northern TP (the NWTP and NETP). Even in the same latitudinal band, the moisture received by the SETP is more than that by the SWTP (Fig. 7a). For all subregions, the maximum moisture uptake occurred 1–2 days before
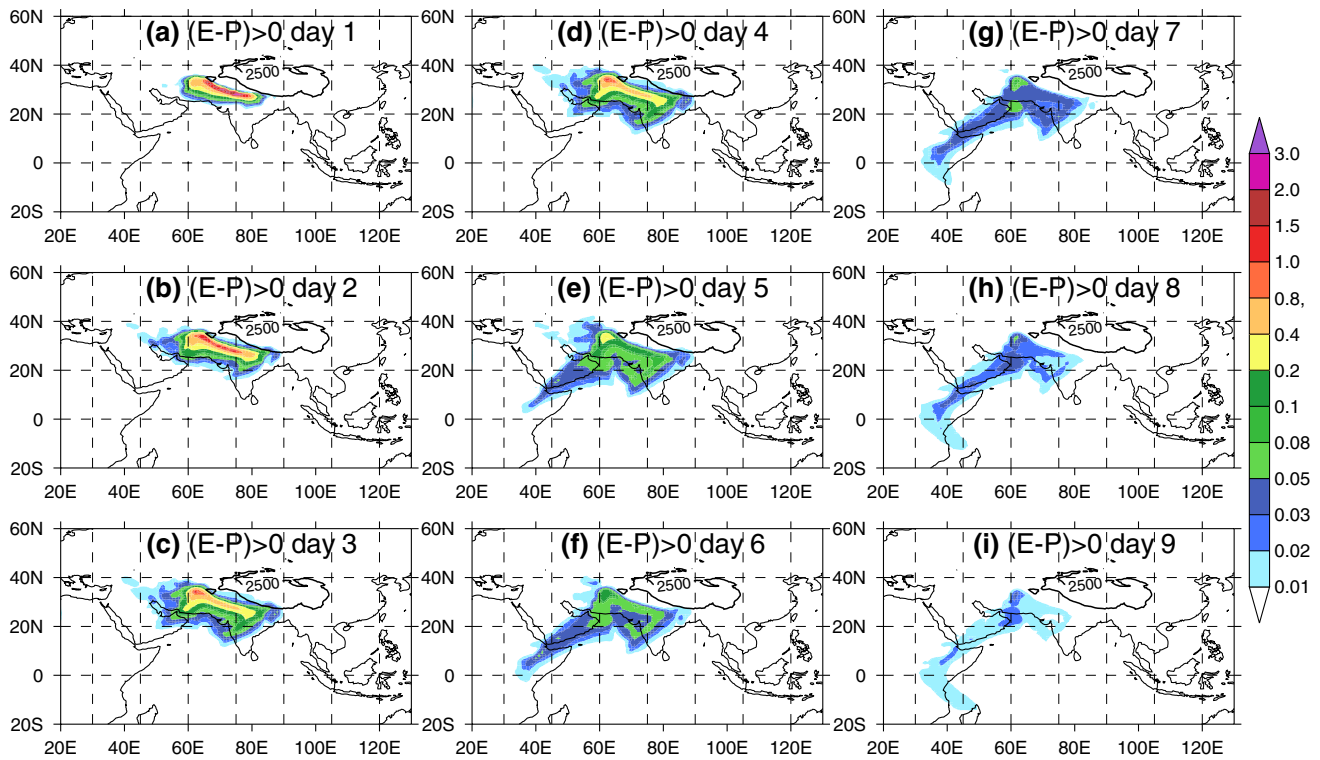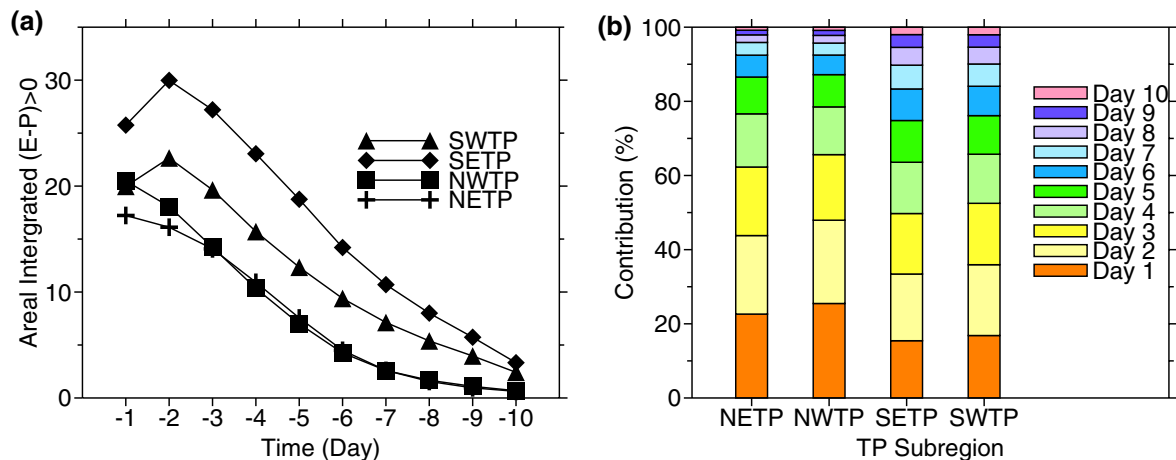
Fig. 5 Same as Fig. 4 but for the SWTP region. *SWTP* southwestern Tibetan Plateau
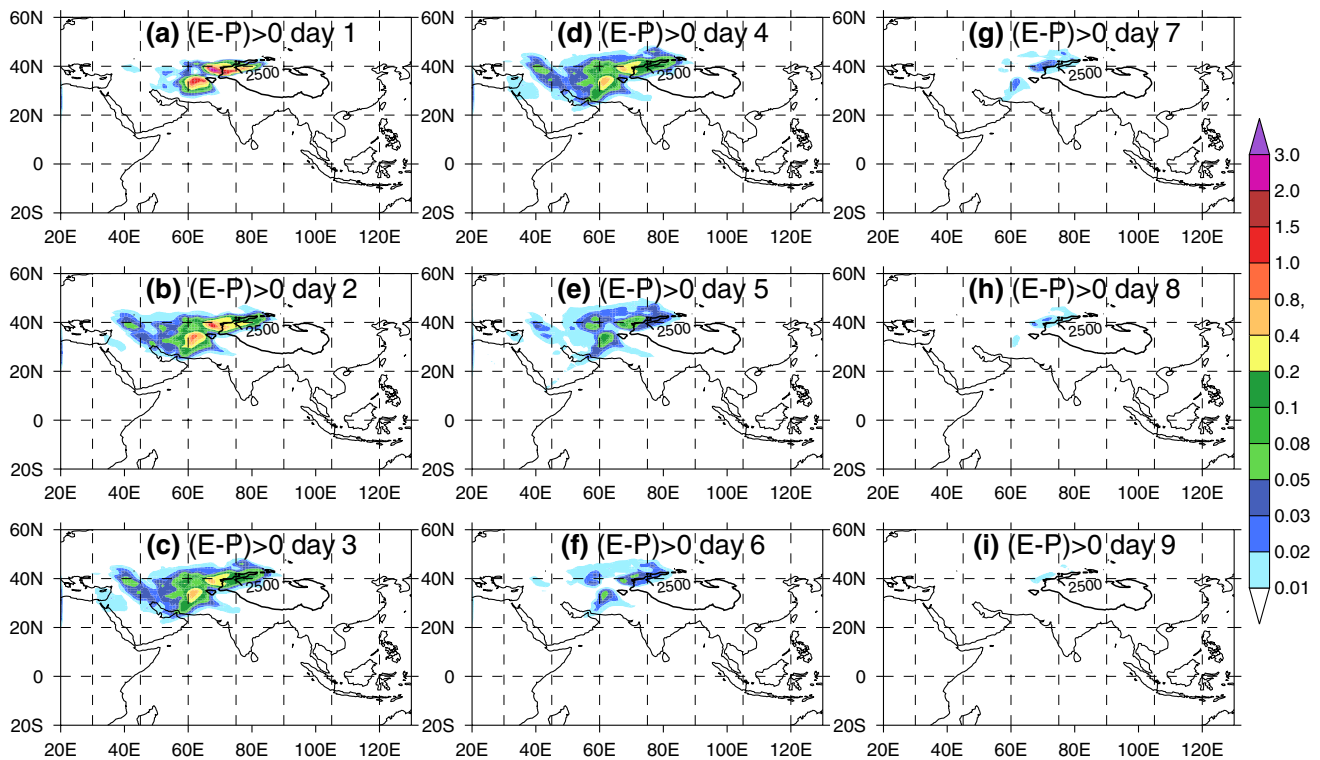
Fig. 6 Same as Fig. 4 but for the NWTP region. *NWTP* northwestern Tibetan Plateau

Fig. 7 **a** The temporal variation in the accumulation of (E–P) > 0 calculated for each separate backward tracking day for the four subregions, and **b** the corresponding relative contribution of all the diagnosed sources of moisture for each of the 10 days

reaching the target regions, implying that considerable moisture from the local or adjacent regions is an important contributor to the water vapor in these target regions during the summer season. Moisture obtained by air mass 1–4 days before reaching the TP contributed ≥ 80% of the moisture in the northern and southern TP, while the contributions of remote moisture sources were less significant. Hence, the moisture sources with relatively shorter transport time scales are the main contributors to the water vapor over the TP.

3.3 Subseasonal variations

To dissect the physical mechanisms controlling the moisture supply in the subregions of the TP, the subseasonal variations and monthly changes in moisture sources within the summer season for individual subregions are further examined. Figure 8 shows the mean sources of the water vapor reaching the southeastern TP (the 10-day integrated (E–P) > 0) from May to August during 1980–2016. Not surprisingly, for the summer months (MJJA), the patterns of moisture sources for the SETP largely overlapped in most areas, particularly over the northern Indian continent and parts of the SETP itself, suggesting that terrestrial moisture sources in Southeast Asia exert the strongest influence. However, there is a significant southwestward shift during the summer season. In early May, the moisture sources with the maximum values greater than 0.2 mm day^{-1} were mainly located over the entire Indian continent, including northern India (Fig. 8a). In June, when the Somali jet and the South Asian summer monsoon started to bring abundant moisture from the Indian Ocean and the Indian subcontinent to the SETP, the moisture source region extended southwestward and covered the Arabian Sea and even the eastern parts of Africa (Fig. 8b). Figure 8a also reveals that the regions west of 60°E between 20°N and 40°N also made a marked contribution to the water

vapor over the SETP. In July, with the migration of the South Asian summer monsoon, the moisture source region expands dramatically further. The moisture supplies from the Tropical Ocean and regions in the Southern Hemisphere increase (Fig. 8c). In August, the spatial distribution of the moisture sources for the SETP remained almost the same, but the main source region shrinks, and the magnitude significantly decreases, especially for the contribution from the Indian continent (Fig. 8d). Obviously, the above monthly changes in moisture sources reflect the subseasonal evolution of the southern Asian monsoon circulation systems. Nevertheless, further studies are required to explore their relationships.

For the SWTP region, the monthly changes in moisture sources (Supplementary Fig. S2) exhibit similar characteristics as those for the SETP region. From May to August, the moisture source regions for the SWTP expand and extend southwestward, accompanied with the development of the summer monsoon. However, the characteristics of the moisture sources for the SETP also differ from those for the SWTP. The majority of the moisture sources with the maximum values for the SWTP are mainly located southwest of the TP and generally remain steady throughout the whole summer, in contrast to the evolution of the prevailing moisture sources for the SETP (Fig. 8). We postulated that this strong and steady source is related to the local topography and the atmospheric circulation regimes over this region, as mentioned in Dong et al. (2016).

For the subseasonal variability in the moisture sources for the NWTP and NETP regions (Supplementary Figs. S3 and S4), the areas of the significant moisture sources expand slightly, and the maximum values generally remained in the same locations from May to August. Although a narrow band stretches from the Arabian Peninsula to Africa (Figs. S3 b, c and S4 b, c), its contribution is negligible compared to the total contributions of all the moisture sources,

Region SETP: Monthly mean (E-P)>0 of day 1-10, 1980-2016
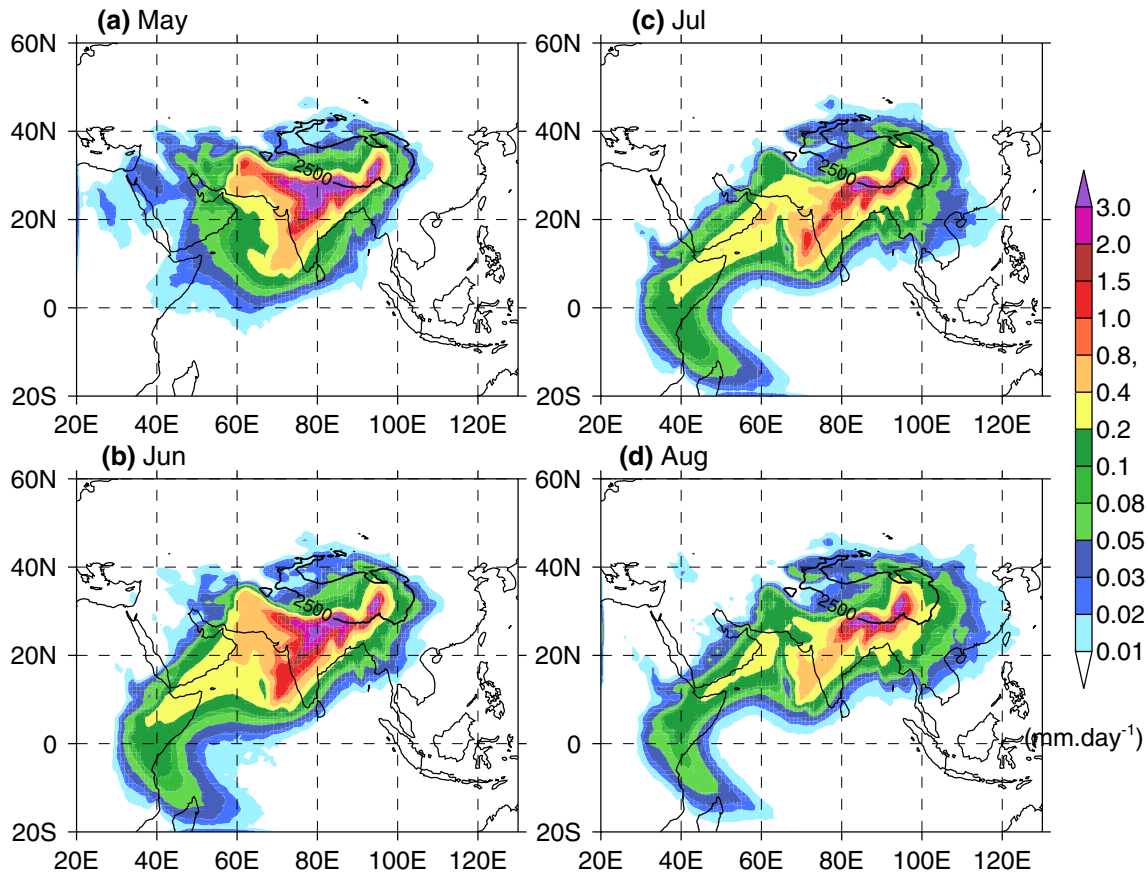
Fig. 8 The monthly averaged moisture sources (namely, the 10-day integrated (E–P) > 0 with units of mm day^{-1}) reaching the southeastern TP region for the months of **a** May, **b** June, **c** July and **d** August, during the period of 1980–2016. The black contour indicates the 2500 m elevation

indicating that the water vapor transported to the northern TP is hardly influenced by the advance and retreat of the Asian summer monsoon during the summer season.

For a better comparison, we calculate the areal integrated moisture sources for each subregion, which are obtained by aggregating all the values of the corresponding moisture sources at a grid point. The daily evolution is shown in Fig. 9. For the southern TP (the SETP and SWTP), the subseasonal variability in moisture sources is significant. In contrast, the monthly changes in moisture sources for the northern TP (the NWTP and NETP) are much less obvious, particularly for the NETP region that features a steady contribution from May to August. These results confirm that the southern TP is influenced by the Asian summer monsoon, whereas the northern TP is hardly influenced by these monsoon systems.

The analysis results show that the SETP and SWTP also exhibit profoundly different subseasonal variability characteristics, even though they are located within the same latitudinal band. The amount of water vapor delivered to the SETP abruptly increases in early May, with peak values
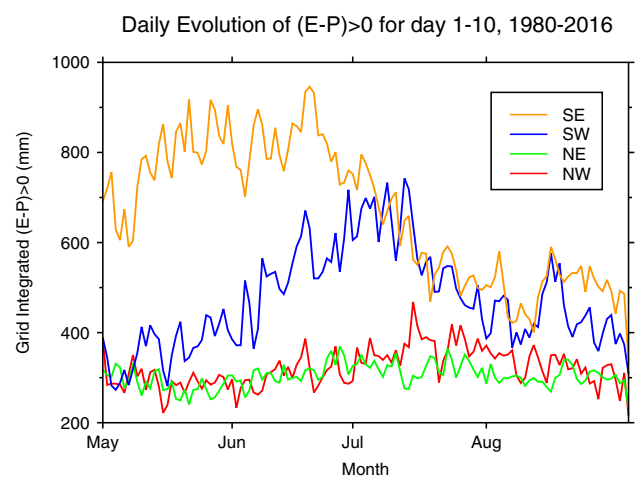
Fig. 9 The daily evolution of the areal integrated moisture sources for the NWTP (red), NETP (green), SWTP (blue), and SETP (orange). The values were obtained by adding all values of the corresponding moisture sources at the grid point

remaining more than 450 mm until the end of June. Then, the moisture source contribution decreases sharply. However, the amount of water vapor transported to the SWTP in early May is relatively low, with the same magnitude as that for the NWTP and NETP. After the middle of May, the moisture contribution increases steadily and peaks in early and middle July and then decreases in the following days, accompanying with the similar-magnitude decrease over the SETP. These differences in the evolution of source contributions can be explained partly by the development of the atmospheric circulation systems that are responsible for the water vapor transport from the sources to the target regions. We speculate that the active deep convection first becomes well developed over the Indian continent in early May (Pathak et al. 2017; Wei et al. 2017), resulting in the Indian summer monsoon. Consequently, the Indian continent becomes a substantial moisture source for the SETP starting in May. Meanwhile, the convection remains relatively weak over the region southwest of the SWTP. Because of the insufficient uplift of water vapor, the moisture cannot be transported to the SWTP through the up-and-over mechanism. In early and middle June, the Indian summer monsoon strengthens further as the deep convection intensifies, and the moisture supply to the SWTP begins to increase, peaking in the middle of July. After that, as the deep convection weakens and the Indian summer monsoon retreats, the contributions to the SWTP and SETP drop.

3.4 Interannual variability and the association with precipitation

Moisture source is closely associated with precipitation changes. In this section, the relationships between the moisture supplies of the TP subregions and corresponding precipitation over the TP are examined and compared. Here, we focus particularly on the interannual variability because it is a crucial benchmark for seasonal rainfall prediction (Ding 1992; Zhou and Yu 2005). Figure 10 shows the interannual variation in the accumulated total moisture supply for the four subregions against the corresponding station-based rainfall derived from NMIC/CMA. The summer moisture supply of the TP is characterized by remarkable interannual variability. With the exception of the moisture supply of the NWTP, the correlation between moisture supply and precipitation is positive. The correlation coefficients between the observed precipitation and the moisture supply for the SETP, SWTP, and NETP are 0.60, 0.40 and 0.39, respectively, which are statistically significant at the 99%, 90% and 90% confidence levels based on Student's t test, whereas the correlation coefficient for the NWTP is -0.22, which is not significant (P = 0.19). Overall, we find that the correlation coefficients between moisture source and precipitation are higher for the southern TP than those for the northern

TP. The positive correlation during the study period implies that the changes in the annual moisture supply contribute substantially to the interannual variability in the observed precipitation. However, the results also suggest that the external sources of moisture to the NWTP are not necessarily coupled to precipitation on the interannual scale.

To further examine the regions that potentially contributed to the precipitation variability, a composite analysis of the anomalies in the moisture sources during the wettest and driest summer seasons was conducted. The years with anomalies in annual precipitation exceeding one standard deviation are selected, and the composite difference in moisture sources between the wettest and driest summer seasons (wettest-driest) for the NWTP, NETP, SWTP, and SETP regions, seperately, were calculated. In the Fig. 11, the positive values indicate the more moisture sources contribution during the periods of wettest summer seasons, and the negative values corresponds to the less moisture sources for the driest season. The interannual variability in the observed summer precipitation over the four TP subregions is generally positively correlated with the moisture from local or nearby terrestrial evaporation (Fig. 11). Therefore, local or neighboring recycling processes make a substantial contribution to the changes in annual precipitation. The role of local cycling in precipitation variability has been documented by Guo et al. (2018), who concluded that the TP has strong regional precipitation systems during the summer season and that locally recycled moisture plays a crucial role in modulating the precipitation over the TP. Moreover, Wang et al. (2017) stressed the roles of local surface evaporation in the variability of summer precipitation over the southern TP. Here, we found that local surface evaporation is significantly higher for wettest seasons.

In addition to the influence of the surrounding areas, remote regions with higher or lower values also modulate the summer precipitation over the TP (Fig. 11). Taking the SETP region as an example (Fig. 11d), the regions with positive values cover the Indian continent, the Arabian Sea, and even the eastern Africa, and is significant at the level of 0.01 (indicated by dots). In contrast, the regions with negative values are mainly located west of the SETP. Associated with the water vapor transport controlled by the southern Asian summer monsoons and the westerlies, the anomalies in the moisture supply over these remote regions modulate the variability in summer rainfall over the SETP. In wet years, the SWTP is less likely to receive moisture from areas to the west and more likely to receive moisture from subtropical or tropical regions. Considering the large regions covered by the remote sources, we also speculate that the interannual variation in summer rainfall across the TP is mainly influenced by the remote moisture supply, which is largely controlled by variability in the large-scale atmospheric circulation patterns, consistent
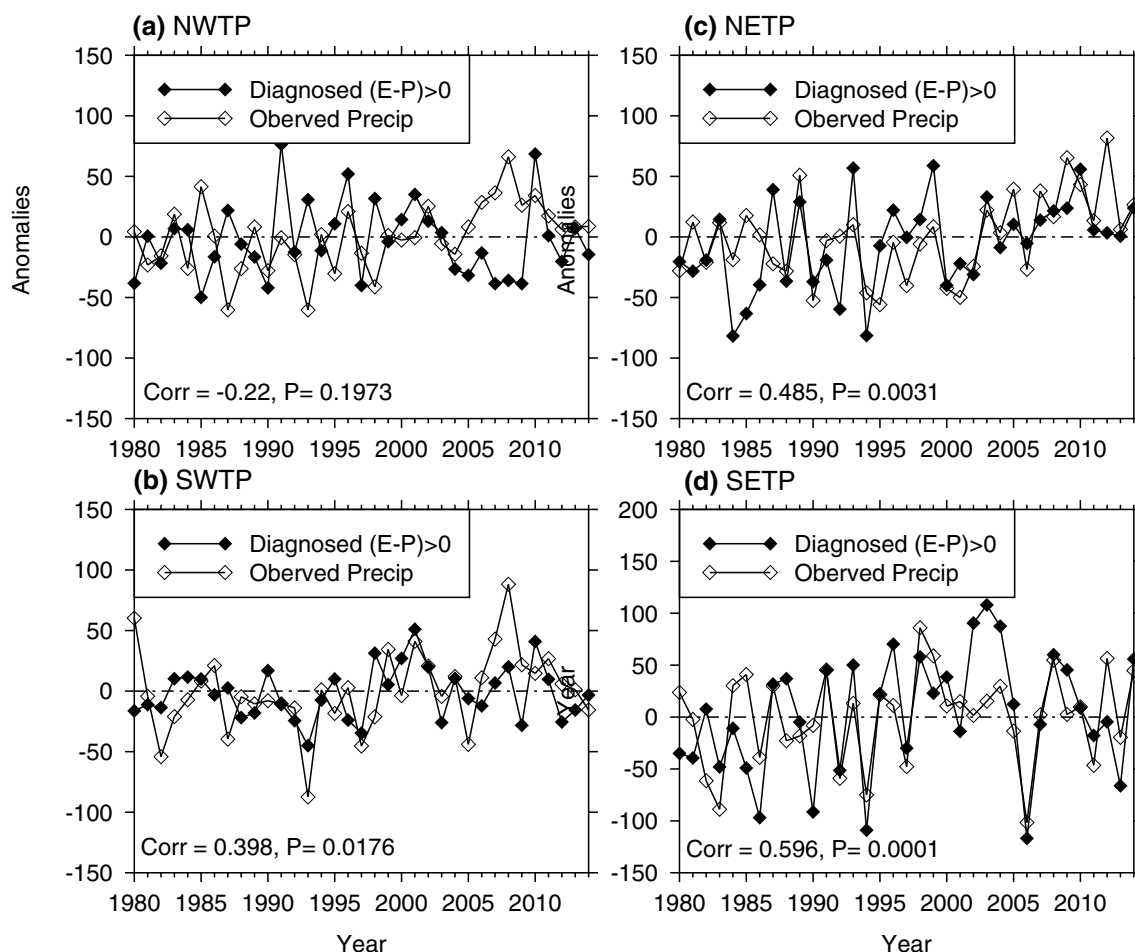
Fig. 10 Time series of station-based summer rainfall from the National Meteorological Information Center of the China Meteorological Administration (units: millimeter per season) over the four subregions of **a** the NWTP, **b** NETP, **c** SWTP, and **d** SETP during 1980–2016 with the corresponding a really determined moisture supplies, which were derived from the Lagrangian backward tracking approach. The correlation coefficient and the significance level are shown in the bottom of the panels

with previous studies (e.g., Chen et al. 2012; An et al. 2017; Wang et al. 2017; Zhang et al. 2019).

In summary, these results indicate that neighborhood recycling and the remote water supply jointly influence the interannual variability of precipitation over the TP. The moisture contributions from neighborhood recycling are positively correlated with precipitation at the interannual time scale. The moisture conveyed by the Indian summer monsoon and the westerlies is positively correlated with precipitation over the southern and northern TP, respectively. These results also offer an additional evidence that the combined effects of high or low moisture supplies associated with the Indian Asian summer monsoon and the high or low moisture supplies associated with the westerlies are responsible for the interannual variability of the summer precipitation over the TP.

4 Discussion

4.1 Comparison of the identified moisture sources with previous studies

A number of previous studies have identified the moisture sources using a wide variety of methods. Although the vast majority of past studies were limited to a single predefined subregion of the TP or a relatively short period, the results presented here are generally consistent with the results of previous studies. For instance, the findings in earlier analyses, such as the importance of local recycling (e.g., Curio et al. 2015; Sun and Wang 2014; Zhang et al. 2017), the differences in dominant atmospheric circulation patterns among the TP subregions (Yao et al. 2013), the
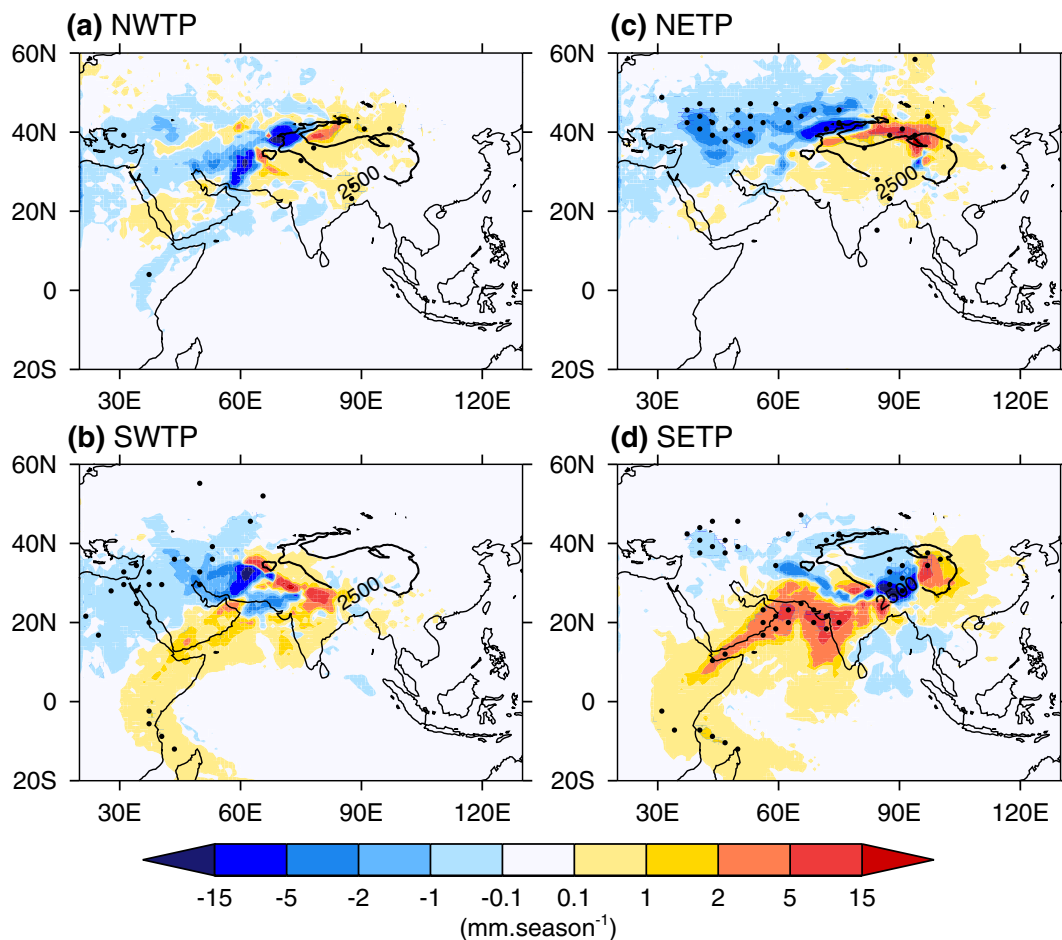
Fig. 11 Difference maps of the anomalies in moisture sources (shading; units: millimeter per season) between the wettest and driest summer seasons for the **a** NWTP, **b** NETP, **c** SWTP, and **d** SETP regions. The wettest and driest years were selected as those with annual precipitation anomalies exceeding one standard deviation. The regions with dots indicate significance at the 95% confidence level

significant contributions of the Eurasian continent to the eastern TP water vapor (Sun and Wang 2014), the abundance of moisture transported from central-eastern India to the southwestern TP (Dong et al. 2016), and the combined effects of the westerlies and local moisture recycling on water supply for the western TP (Yao et al. 2013), are further verified by our results.

In addition to this agreement, the results presented here also exhibit some discrepancies with earlier analyses. For instance, we found that the contribution of the East Asian monsoon is not significant, which is somewhat different from the conclusions of previous studies. Feng and Zhou (2012) indicated that the Bay of Bengal was one of most important sources of moisture for the TP during the summer. However, our analysis detected no water vapor from this region, consistent with the results of Curio et al. (2015). This discrepancy might be associated with the differences in the study period. The Bay of Bengal monsoon develops in early May before the Indian monsoon from

the southern Indian Ocean and might be another major moisture source.

More recently, Zhang et al. (2017) highlighted that the moisture sourced from the Eurasian continent and local surface evaporation made a greater contribution to the precipitation over the western-central TP. Pan et al. (2018) also showed that the dominant moisture source for precipitation over the southern TP is tropical Indian oceanic areas. Compared to those analyses, the moisture sources identified in this study covered less extensive areas, especially for remote regions. Despite the different data sets used in the studies, this underestimation of the remote moisture sources could be partly due to the two following aspects. On one hand, the water accounting method used in Zhang et al. (2017) assumed that the precipitation was well mixed throughout the atmospheric column. However, in reality, the majority of water vapor resides in the lower level of the atmosphere. On the other hand, the strong wind associated with the westerlies over
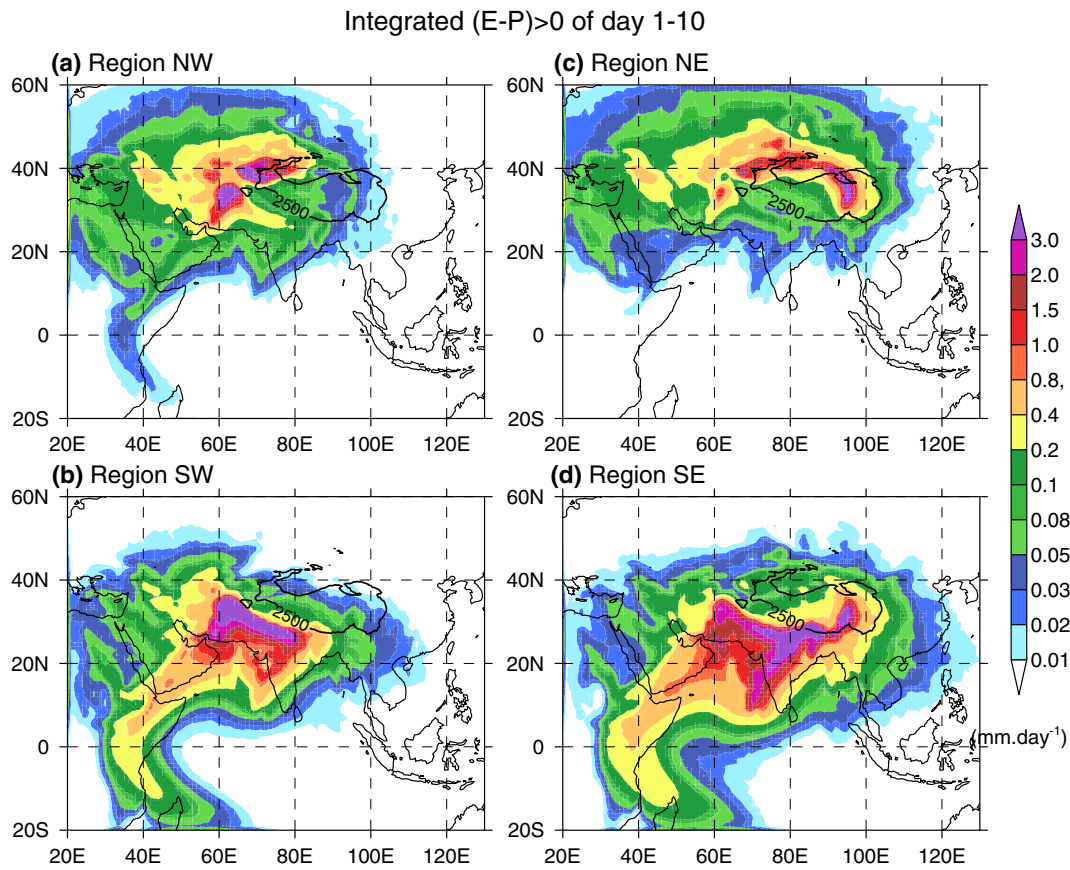
Integrated (E-P)>0 of day 1-10

Fig. 12 Same as Fig. 2 but without consideration of multiple cycles of precipitation

the northern TP can introduce more water supplies from the land. The approach adopted by this study considers multiple cycles of precipitation processes for each air parcel. Similar to Fig. 3, the climatology of summer average moisture sources is shown in Fig. 12, but without consideration of the multiple cycles of precipitation processes.

The moisture source regions clearly have larger areas and markedly higher values, especially in the remote moisture regions.

The relative contributions of all the identified sources of moisture over a 10-day period are presented but not rescaled in Fig. 13. The comparison of Fig. 13 with Fig. 7 further
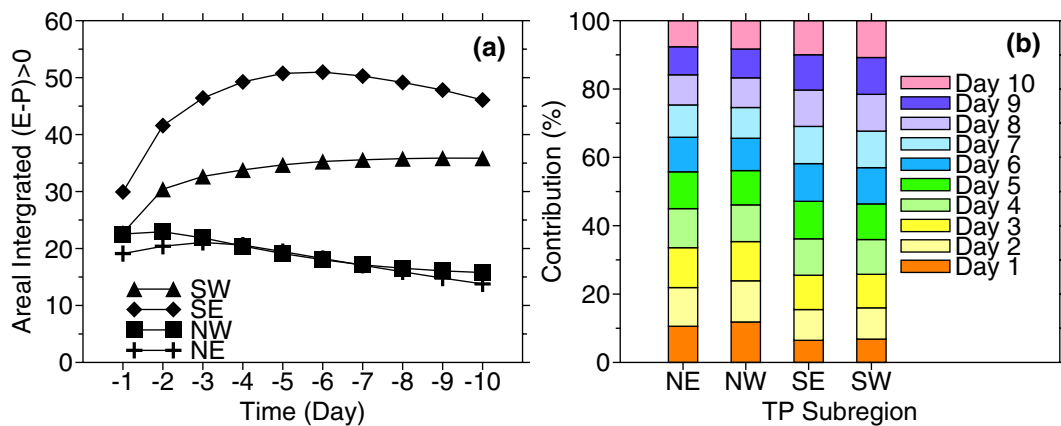

Fig. 13 Same as Fig. 7 but without consideration of multiple cycles of precipitation

shows that if the multiple precipitation cycles are not taken into account, the fractional contributions of sources with longer transport time increase. In this analysis, the contributions on the tenth day increase from 26.1 to 51.4% and from 11.8 to 22.2%. These sharp increases in contribution imply that a large amount of the moisture in the air parcels is lost through precipitation during transport to the target region (Sun and Wang 2014). However, the aforementioned studies did not account for the associated gains/losses of moisture over the target regions. Moreover, in this study, the moisture sources were identified for the water vapor rather than for precipitation as by Zhang et al. (2017), and this difference could be another factor that contributes to different results.

4.2 Relationship between moisture supply and interannual variability in precipitation

The analysis in this study confirmed that the moisture supply from neighboring regions or local recycling provides more water vapor for precipitation than the regions far from the TP, particularly for the northern TP (Fig. 7; Curio et al. 2015). However, the remote moisture contributions driven by large-scale atmospheric circulation patterns play the leading role in influencing the interannual variability of summer precipitation over the TP (Feng and Zhou 2012; Wang et al. 2017). The results of this study regarding the importance of different subregions, however, appear to differ slightly from those of the recent study by Wang et al. (2017), who suggested that the precipitation over the southern TP is primarily influenced by moisture transport at the western boundary and that the moisture inflow at the southern boundary is secondary. However, our analysis shows that the moisture transported from the western remote regions to the SWTP and SETP is negatively correlated with the precipitation over the TP (Fig. 11). Note that, we only concentrated on the moisture that reaches the subregions of the TP (Fig. 1), which is considerably different from the predefined boundaries of the southern TP by Zhang et al. (2017). This discrepancy hinders a direct comparison, and further analysis is required.

For the NWTP, the relationship between moisture source and precipitation at the interannual scale is rather weak. We postulate that this weak relationship might be due to the complex mechanisms of precipitation formation in this region. Precipitation in this region could be impacted by the Indian monsoon, the westerlies and local cycling. Previous results showed that on average, almost half of the precipitation over the NWTP is supplied by regional moisture recycling (An et al. 2017). Moreover, stronger westerly winds also bring a fraction of moisture from the Mediterranean to this region. Therefore, precipitation in this region is subject to strong spatial–temporal variations. Furthermore, intensification of local recycling and weakening of the Indian monsoon could also weaken the relationship between source area

variability and precipitation at the interannual scale (Worden et al. 2007).

4.3 Uncertainties associated with the methods

Stohl and James (2004) and Gimeno (2012) summarized the main disadvantages of the Lagrangian method for moisture source determination. In addition to the limitations of the Lagrangian model, other sources of errors include the limited resolution and interpolation of the input data. Compared to the accuracies of methods used in other studies, the accuracy of the relatively sophisticated method used in this study mainly depends on the accuracy of the trajectories. Because of the harsh conditions and sparse gauging stations on the TP, we separated the homogenous regional atmosphere into more than 1.4 million air parcels. This enormous number of trajectories can reduce the errors to some extent (Stohl and James 2004). In addition, although it should be noted that the interpretation of the results is only applied to the "ERA-Interim world", the ERA-Interim reanalysis performs better than other reanalysis data sets in simulating the atmospheric water budget over the TP (Gao et al. 2014; Zhang et al. 2017). Moreover, the relatively high resolution of $0.75° × 0.75°$ in the ERA-Interim data set also enhances the accuracy of the trajectory calculation.

5 Summary and conclusions

This study has attempted, for the first time, to identify and compare the moisture sources for four TP subregions over the period 1980–2016. A relatively sophisticated Lagrangian algorithm was employed to identify the climatological moisture sources of water vapor reaching the four TP subregions during the summer season (May–August) of 1980–2016. The transport characteristics, subseasonal variability and their relevance to the precipitation changes at the interannual scale were also analyzed and compared. Owing to the inherent topographical features of the four subregions and the controlling atmospheric circulation patterns, the patterns of the moisture sources for the four subregions exhibit significant differences, both in spatial pattern and magnitude. The results provide insights into the origin of atmospheric moisture and the underlying processes, such as evaporation and condensation. The main findings are summarized as follows:

1. Climatologically, the neighboring or adjacent regions are one of the main moisture sources during the summer season for all subregions during May–August. The remote sources of water vapor reaching the northern TP is mainly concentrated on the Eurasian continent, which is dominated by the westerlies, and the contributions

from the lower latitudinal regions are almost negligible. However, for the southern TP, immense subtropical and tropical areas tend to be the predominant contributors because of the influence of the Indian summer monsoon.

2. The water supply of the TP is dominated by the moisture transported within 1–4 days before arrival, accounting for approximately 80% of the total moisture transport. However, the moisture transport to the northern TP within 5–10 days is steady over the neighboring regions, in contrast to the southern TP that features a long-distance transport from subtropical and tropical regions. These results confirm the importance of the moisture contributions of neighboring regions and the Indian summer monsoon to the northern and southern TP, respectively.

3. The moisture sources for the southern TP exhibit subseasonal variations in the contributions from different sources during summer, whereas the subseasonal variation in the northern TP is not significant. The subseasonal migration of the Indian summer monsoon is an important component regulating the relative importance of different sources for the southern TP, but this is not the case for the northern TP. Even within the same latitudinal belt, the subseasonal evolution of the moisture sources for the southeastern TP differs greatly from that for the southwestern TP.

4. At the interannual scale, moisture supply is obviously associated with precipitation in three of the four subregions of the TP, with the exception of the NWTP region. Neighborhood recycling and remote water supply jointly influence the year-to-year variability of precipitation over the TP. Precipitation is negatively correlated with remote water supply conveyed by the westerlies, while it is positively correlated with moisture supply conveyed by the Indian summer monsoon in the northern TP and by neighboring transport in the southern TP.

The results discussed herein provide a climatological overview of moisture sources for the subregions of the TP. However, the linkage between atmospheric moisture transport and precipitation across the TP remains poorly established. There is lack of analysis on the extreme modes of climate variability, such as the El Niño-Southern Oscillation (ENSO) or the North Atlantic Oscillation, which have been shown to affect precipitation variability over the TP. The long period of data in this study allows to explore the interannual variability of moisture sources and its relationship with the major climate modes. Such analysis will form part of a future study.

References

An W, Hou S, Zhang Q, Zhang W, Wu S, Xu H, Pang H, Wang Y, Liu Y (2017) Enhanced recent local moisture recycling on the Northwestern Tibetan Plateau deduced from ice core deuterium excess records. J Geophys Res Atmos 122(23):12541–512556

Bibi S, Wang L, Li X, Zhou J, Chen D, Yao T (2018) Climatic and associated cryospheric, biospheric, and hydrological changes on the Tibetan Plateau: a review. Int J Climatol 38(S1):e1–e17

Bolch T et al (2012) The state and fate of Himalayan Glaciers. Science 336(6079):310

Bookhagen B, Burbank DW (2010) Toward a complete Himalayan hydrological budget: spatiotemporal distribution of snowmelt and rainfall and their impact on river discharge. J Geophys Res 115:F03019. https://doi.org/10.1029/2009JF001426

Bothe O, Fraedrich K, Zhu XH (2012) Tibetan Plateau summer precipitation: covariability with circulation indices. Theor Appl Climatol 108:293–300

Chen B, Xu XD (2016) Spatiotemporal structure of the moisture sources feeding heavy precipitation events over the Sichuan Basin. Int J Climatol 36(10):3446–3457

Chen B, Xu XD, Yang S, Zhang W (2012) On the origin and destination of atmospheric moisture and air mass over the Tibetan Plateau. Theor Appl Climatol 110(3):423–435

Chen B, Xu XD, Zhao T (2018) Quantifying oceanic moisture exports to mainland China in association with summer precipitation. Clim Dyn 51(11):4271–4286

Curio J, Maussion F, Scherer D (2015) A 12-year high-resolution climatology of atmospheric water transport over the Tibetan Plateau. Earth Syst Dyn 6(1):109–124

Dee DP et al (2011) The ERA-Interim reanalysis: configuration and performance of the data assimilation system. Q J R Meteorol Soc 137(656):553–597

Ding Y (1992) Summer monsoon rainfalls in China. J Meteorol Soc Jpn 70(1B):373–396

Dong W et al (2016) Summer rainfall over the southwestern Tibetan Plateau controlled by deep convection over the Indian subcontinent. Nat Commun 7:10925

Drumond A, Nieto R, Gimeno L, Ambrizzi T (2008) A Lagrangian identification of major sources of moisture over Central Brazil and La Plata Basin. J Geophys Res Atmos 113(D14):D14128

Feng L, Zhou T (2012) Water vapor transport for summer precipitation over the Tibetan Plateau: multidata set analysis. J Geophys Res Atmos 117(D20):D20114

Gao Y, Cuo L, Zhang Y (2014) Changes in moisture flux over the Tibetan Plateau during 1979–2011 and possible mechanisms. J Clim 27(5):1876–1893

Gimeno L, Drumond A, Nieto R, Trigo RM, Stohl A (2010a) On the origin of continental precipitation. Geophys Res Lett 37:L13804. https://doi.org/10.1029/2010GL043712

Gimeno L, Nieto R, Trigo RM, Vicente-Serrano SM, Lopez-Moreno JI (2010b) Where does the Iberian Peninsula moisture come from? An Answer Based on a Lagrangian Approach. J Hydrometeorol 11(2):421–436

Gimeno L, Stohl A, Trigo RM, Dominguez F, Yoshimura K, Yu L, Drumond A, Durán-Quesada AM, Nieto R (2012) Oceanic and

terrestrial sources of continental precipitation. Rev Geophys. https://doi.org/10.1029/2012rg000389

Guo L, Klingaman NP, Demory M-E, Vidale PL, Turner AG, Stephan CC (2018) The contributions of local and remote atmospheric moisture fluxes to East Asian precipitation and its variability. Clim Dyn 51(11):4139–4156

Immerzeel WW, van Beek LPH, Bierkens MFP (2010) Climate change will affect the Asian water towers. Science 328(5984):1382–1385

Li M, Babel W, Tanaka K, Foken T (2013) Note on the application of planar-fit rotation for non-omnidirectional sonic anemometers. Atmos Meas Tech 6(2):221–229

Ma Y, Yao T, Wang J (2006) Experimental study of energy and water cycle in Tibetan Plateau—the progress introduction on the study of GAME/Tibet and CAMP/Tibet. Plateau Meteorol 25(2):344–351

Ma Y, Lu M, Chen H, Pan M, Hong Y (2018) Atmospheric moisture transport versus precipitation across the Tibetan Plateau: a mini-review and current challenges. Atmos Res 209:50–58

Maussion F, Scherer D, Mölg T, Collier E, Curio J, Finkelnburg R (2014) Precipitation seasonality and variability over the Tibetan Plateau as resolved by the high Asia reanalysis. J Clim 27(5):1910–1927

Nieto R, Duran-Quesada AM, Gimeno L (2010) Major sources of moisture for Antarctic ice-core sites identified through a Lagrangian approach. Clim Res 41(1):45–49

Numaguti A (1999) Origin and recycling processes of precipitating water over the Eurasian continent: experiments using an atmospheric general circulation model. J Geophys Res Atmos 104(D2):1957–1972

Pan C, Zhu B, Gao J, Kang H, Zhu T (2019) Quantitative identification of moisture sources over the Tibetan Plateau and the relationship between thermal forcing and moisture transport. Clim Dyn 52:181–196

Pathak A, Ghosh S, Martinez JA, Dominguez F, Kumar P (2017) Role of oceanic and land moisture sources and transport in the seasonal and interannual variability of summer monsoon in India. J Clim 30(5):1839–1859

Sodemann H, Schwierz C, Wernli H (2008) Interannual variability of Greenland winter precipitation sources: Lagrangian moisture diagnostic and North Atlantic Oscillation influence. J Geophys Res Atmos 113(D3):D03107

Stohl A, James P (2004) A Lagrangian analysis of the atmospheric branch of the global water cycle. Part I: method description, validation, and demonstration for the August 2002 flooding in Central Europe. J Hydrometeorol 5(4):656–678

Stohl A, James P (2005) A Lagrangian analysis of the atmospheric branch of the global water cycle. Part II: moisture transports between earth's ocean basins and river catchments. J Hydrometeorol 6(6):961–984

Sun B, Wang H (2014) Moisture sources of semiarid grassland in China using the Lagrangian particle model FLEXPART. J Clim 27(6):2457–2474

Wang Z, Duan A, Yang S, Ullah K (2017) Atmospheric moisture budget and its regulation on the variability of summer precipitation over the Tibetan Plateau. J Geophys Res Atmos 122(2):614–630

Wang X, Pang G, Yang M (2018) Precipitation over the Tibetan Plateau during recent decades: a review based on observations and simulations. Int J Climatol 38(3):1116–1131

Wei W, Zhang R, Wen M, Yang S (2017) Relationship between the Asian Westerly Jet Stream and summer rainfall over Central Asia and North China: roles of the Indian Monsoon and the South Asian High. J Clim 30(2):537–552

Worden J et al (2007) Importance of rain evaporation and continental convection in the tropical water cycle. Nature 445:528

Wu G, Liu Y, Zhang Q, Duan A, Wang T, Wan R, Liu X, Li W, Wang Z, Liang X (2007) The influence of mechanical and thermal forcing by the Tibetan Plateau on Asian Climate. J Hydrometeorol 8(4):770–789

Xu X, Lu C, Shi X, Gao S (2008) World water tower: an atmospheric perspective. Geophys Res Lett 35:L20815. https://doi.org/10.1029/2008GL035867

Xu X, Zhao T, Lu C, Guo Y, Chen B, Liu R, Li Y, Shi X (2014) An important mechanism sustaining the atmospheric "water tower" over the Tibetan Plateau. Atmos Chem Phys 14(20):11287–11295

Yang K, Wu H, Qin J, Lin C, Tang W, Chen Y (2014) Recent climate changes over the Tibetan Plateau and their impacts on energy and water cycle: a review. Glob Planet Chang 112:79–91

Yao T et al (2013) A review of climatic controls on $\delta^{18}O$ in precipitation over the Tibetan Plateau: observations and simulations. Rev Geophys 51(4):525–548

Zhang C, Tang Q, Chen D (2017) Recent changes in the moisture source of precipitation over the Tibetan Plateau. J Clim 30(5):1807–1819

Zhang C, Tang Q, Chen D, van der Ent RJ, Liu X, Li W, Haile GG (2019) Moisture source changes contributed to different precipitation changes over the northern and southern Tibetan Plateau. J Hydrometeor 20:217–229

Zhong L, Ma Y, Hu Z, Fu Y, Hu Y, Wang X, Cheng M, Ge N (2019) Estimation of hourly land surface heat fluxes over the Tibetan Plateau by the combined use of geostationary and polar-orbiting satellites. Atmos Chem Phys 19(8):5529–5541

Zhou T-J, Yu R-C (2005) Atmospheric water vapor transport associated with typical anomalous summer rainfall patterns in China. J Geophys Res 110:D08104. https://doi.org/10.1029/2004JD005413